Adhesive Layer-by-Layer Films of Carboxymethylated Cellulose Nanofibril–Dopamine Covalent Bioconjugates Inspired by Marine Mussel Threads

Erdem Karabulut,[†] Torbjörn Pettersson,[†] Mikael Ankerfors,[‡] and Lars Wågberg[†,§,*]

[†]Fibre and Polymer Technology, KTH Royal Institute of Technology, Teknikringen 56, SE 10044 Stockholm, Sweden, [‡]Material Processes, Innventia AB, Box 5604, 11486 Stockholm, Sweden, and [§]Wallenberg Wood Science Centre, Teknikringen 56, 10044, Stockholm, Sweden

ABSTRACT The preparation of multifunctional films and coatings from sustainable, low-cost raw materials has attracted considerable interest during the past decade. In this respect, cellulose-based products possess great promise due not only to the availability of large amounts of cellulose in nature but also to the new classes of nanosized and well-characterized building blocks of cellulose being prepared from trees or annual plants. However, to fully utilize the inherent properties of these nanomaterials, facile and also sustainable preparation routes are needed. In this work, bioinspired hybrid conjugates of carboxymethylated cellulose nanofibrils (CNFC) and dopamine (DOPA) have been prepared and layer-by-layer (LbL) films of these modified nanofibrils have been built up in combination with a branched polyelectrolyte, polyethyleneimine (PEI), to obtain robust, adhesive, and wet-stable nanocoatings on solid surfaces. It is shown that the chemical functionalization of CNFCs with DOPA molecules alters their conventional properties both in liquid dispersion and at the interface and also influences the LbL film formation by reducing the electrostatic interaction. Although the CNFC–DOPA conjugates show a lower colloidal stability in aqueous dispersions due to charge suppression, it was possible to prepare the LbL films through the consecutive deposition of the building blocks. Adhesive forces between multilayer films prepared using chemically functionalized CNFCs and a silica probe are much stronger in the presence of Fe^{3+} than those between a multilayer film prepared from unmodified nanofibrils and a silica probe. The present work demonstrates a facile way to prepare chemically functionalized cellulose nanofibrils whereby more extended applications can produce novel cellulose-based materials with different functionalities.

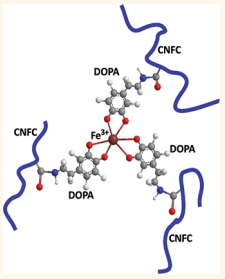

KEYWORDS: adhesion · nanofibrillated cellulose · chemical functionalization · dopamine · layer-by-layer assembly

The design of sustainable functional nanomaterials from renewable sources has attracted considerable interest during recent years both because they are able to mimic "well-designed" materials in nature and because of the need to use our natural resources in a sustainable way. Wood- and cellulose-based materials have been extensively investigated in order to build up novel materials with which to replace petroleum-based products.[1,2] Among these materials, carboxymethylated cellulose nanofibrils (CNFCs),[3–5] with a diameter of 3–7 nm and a length of 1–2 μm, have a high potential to produce materials for many application areas such as functional surface coatings, separation membranes, packaging and insulation, etc. The unique properties of CNFCs such as high strength[6] and high length-to-diameter ratio[7] allow for the preparation of multifunctional materials such as model surfaces,[8] thin films,[9] nanopaper,[6,10] foams,[11] and aerogels[12] with very high porosity. However, limitations such as their hydrophilicity and weak wet stability in liquid media need to be addressed in order to extend their applications. Although the preparation of several types of CNFC-based materials has been reported,[13–15] a limited number of investigations have been reported on materials prepared using chemically functionalized CNFCs. Nanocomposites of cellulose nanofibrils modified with biofunctional organic molecules could show interesting features not typical of the material itself, such as strong adhesion under wet conditions, extensibility, and cross-linking ability. Biological molecules with special functional properties can constitute a convenient route to prepare functional nanomaterials if they are combined with CNFCs in a proper way. In the early 1980s, a protein containing large amounts of lysine, 3,4-dihydroxyphenylalanine (DOPA), and 4-hydroxyproline molecules and produced in the byssus-secreting foot of marine mussels was extracted and it was found that the composition of this protein

* Address correspondence to wagberg@kth.se.

Received for review November 28, 2011 and accepted May 26, 2012.

Published online May 29, 2012
10.1021/nn204620j

played an important role in the adhesion of these organisms to wet surfaces.[16,17] The outer cuticles of the byssal threads of marine mussels exhibit high stiffness and extensibility as well as a strong adhesion to many types of surfaces showing different surface properties.[18−21] Moreover, ionic coordination bonds between DOPA molecules through a transition metal ion, notably Fe^{3+}, in the mussel cuticle improves the hardness and adhesion of the mussel threads.[22−24] The influence of Fe^{3+} ions on the formation of catecholato-iron complexes in the byssus cuticle was demonstrated using resonance Raman spectroscopy, and a model was presented in which the density of these complexes determines the hardness and extensibility of the mussel threads.[25] The surface force apparatus method was used to study the bridging between positively charged mfp-1 protein-coated surfaces, and it was found that the formation of catecholato-iron complexes strongly depended on the Fe^{3+} concentration in the water.[26] Finally, antibacterial layer-by-layer (LbL) films of hyaluronic acid and polyethyleneimine (PEI) modified with catechol-containing molecules were prepared on hydrophobic surfaces in which silver nanoparticles were formed by the redox activity of the catechol groups.[27]

In the present work, we aim to prepare biohybrid conjugates of carboxymethylated cellulose nanofibrils and dopamine (CNFC−DOPA) using the water-soluble carbodiimide activation technique[28] and to build up hierarchical adhesive LbL coatings with properties resembling mussel adhesion on solid substrates. The influences of DOPA grafting on the surface and colloidal properties of CNFC are discussed by both monitoring the LbL film formation of CNFC−DOPA/PEI and comparing the colloidal stability of the conjugate with that of unmodified nanofibrils. The adhesion between a silica particle and the multilayer films of CNFC−DOPA is measured in water and NaCl and $FeCl_3$ solutions, and the influence of catecholato-iron complexation (see Figure 1) on the adhesion is discussed.

RESULTS AND DISCUSSIONS

DOPA Functionalization of CNFC. The covalent conjugation of the DOPA molecules at the nanofibril surface was monitored using FTIR and UV−vis spectroscopy. Figure 2 shows the FTIR spectra of pure CNFC and of CNFC−DOPA covalent hybrids prepared in the presence of water-soluble carbodiimide (EDC) as cross-linker. The broad IR bands between 3000 and 3600 cm^{-1} detected in both modified and unmodified nanofibrils are assigned to the stretching vibrations of −OH and −CH groups on the cellulose backbone. A series of weak bands from 1280 to 1500 cm^{-1} were attributed to −OCH deformation vibrations, $-CH_2$ bending vibrations, and −CCH and −COH bending

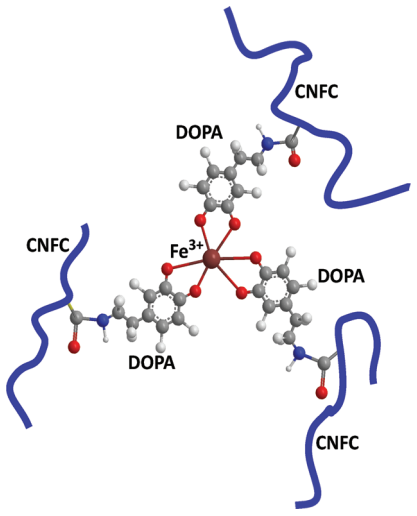

Figure 1. Schematic illustration of catecholato-iron chelate complex formation between CNFC−DOPA and Fe^{3+} ions.

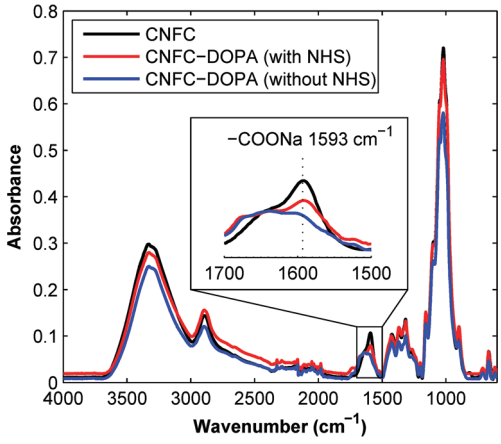

Figure 2. FTIR spectra of pure CNFC (black), CNFC−DOPA conjugate prepared with EDC and NHS (red), and CNFC−DOPA conjugate prepared with EDC (blue).

vibrations. The band ranging from 1200 to 920 cm^{-1} contains mainly the signals of −CC stretching vibrations and −COH and −CCH deformation vibrations. The most distinct difference between the spectra was observed at 1593 cm^{-1}, which corresponds to the asymmetric stretching vibrations of the deprotonated carboxyl groups, since the coupling reaction causes the formation of an amide bond between the carboxyl and amine groups. The spectra show that the intensity of the free carboxyl vibration decreased with DOPA modification, while new IR bands attributed to amide I (amide carbonyl stretching vibrations) vibrations appear at 1680−1630 cm^{-1}. It is well known that the addition of *N*-hydroxysuccinimide (NHS) or its charged analogue sulfo-NHS to such a reaction mixture can enhance the yield under some conditions by the formation of a stable amine-reactive ester intermediate.[29] Therefore, to study the influence of such a modification reagent on the coupling yield, a batch of CNFC−DOPA was synthesized with the

addition of a moderate amount of NHS. As can be seen in Figure 2, the addition of NHS had a negligible effect on the reaction yield since the intensity of the free carboxyl band decreased much more in the case of the batch prepared with no NHS.

UV–vis spectroscopy was used for establishing the CNFC–DOPA covalent conjugate formation. Figure 3 shows the UV–vis spectra of pure CNFC, DOPA, and CNFC–DOPA hybrid conjugate. It is known that the DOPA molecules absorb UV radiation at 220 and 281 nm due to $\pi-\pi^*$ and L_a-L_b coincident transition,[30] whereas no similar absorption bands are observed in the pure cellulose nanofibril dispersion.[31] In this wavelength range, absorption bands corresponding to the DOPA molecules were observed in the case of the dispersion of the CNFC–DOPA conjugate after dialysis against Milli-Q water. The absence of any UV peak relating to the condensing agent and byproduct formed in the reaction indicates that all these compounds were substantially removed in the dialysis step. The degree of DOPA attachment can be estimated by integrating the area under the UV spectrum of CNFC–DOPA, as there is no contribution to the absorbance from pure cellulose in this region. The maximum absorbance of the CNFC–DOPA conjugate prepared by adding an excess amount of DOPA (0.1 mmol) was recorded and used as the reference absorbance value (A_{max} = 0.042) for the other initial amounts of DOPA added to the reaction mixture. In order to calculate the conversion ratio of free carboxylic groups to their DOPA forms, the A_{max} value for the reference conjugate at 281 nm was compared with that of the CNFC–DOPA conjugate prepared using 0.06 mmol of DOPA. The DOPA attachment degree was found to be *ca.* 63%, which means 0.038 mmol of DOPA was grafted to the CNFC. Since the total charge of CNFC is already known, (0.515 mmol g^{-1},[5] as determined by conductometric titration), the reaction yield was found to be *ca.* 76%. The UV–vis spectra of other CNFC–DOPA conjugates prepared using different initial amounts of DOPA are shown in the Supporting Information (Figure S7).

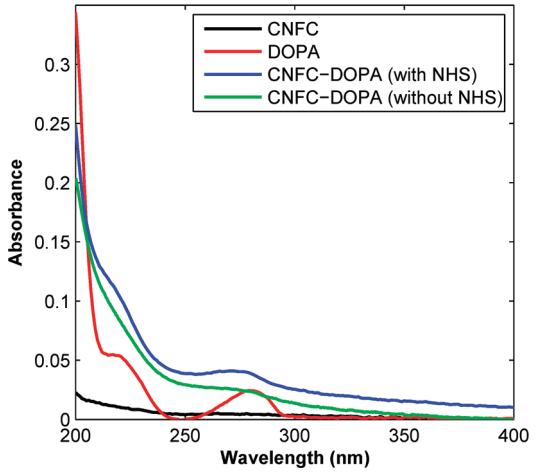

Figure 3. UV–vis spectra of pure CNFC (100 mg L^{-1}) (black), DOPA (8.7 × 10^{-3} mM) (red), and CNFC–DOPA conjugate (100 mg L^{-1}) prepared with EDC/NHS (blue).

Influence of DOPA Modification on the Colloidal Stability of CNFC. Since the DOPA functionalization involves the carboxyl groups on the CNFC, it may be anticipated that the colloidal stability of the fibrils is adversely affected as they are electrostatically stabilized in aqueous dispersions.[32] To clarify this, the colloidal properties of the DOPA-modified nanofibrils were characterized using dynamic light scattering (DLS), a method recently found to be a suitable for determining the stability of CNFC dispersions.[32] Figure 4b shows the average size distribution of pure CNFC and the CNFC–DOPA conjugate in water. The average hydrodynamic diameter (R_h) of nonmodified CNFCs was estimated to be 160 nm, but it was 1.8 μm for CNFC–DOPA, which is approximately 10 times greater

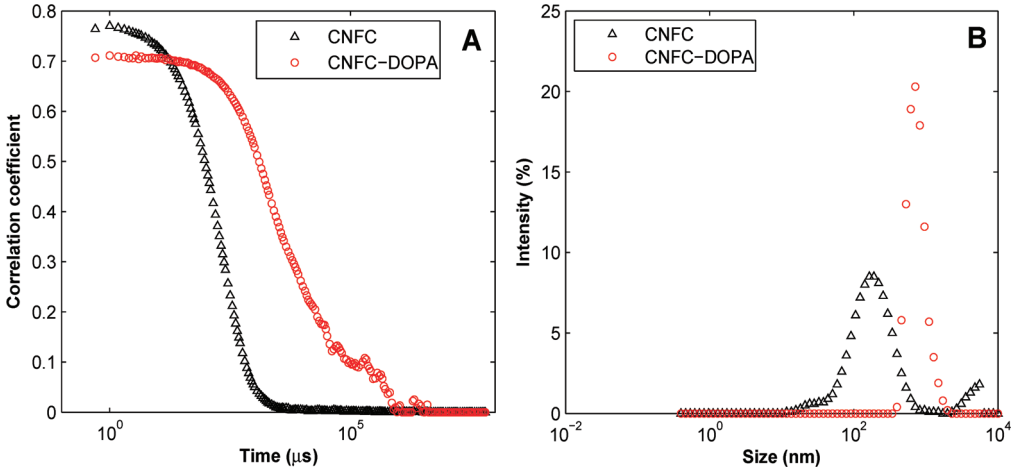

Figure 4. Results from DLS characterization of nonmodified and DOPA-modified CNFC. (a) Autocorrelation function for the pure CNFC and the CNFC–DOPA conjugate. (b) Average particle size distribution of the pure CNFC and CNFC–DOPA conjugate.

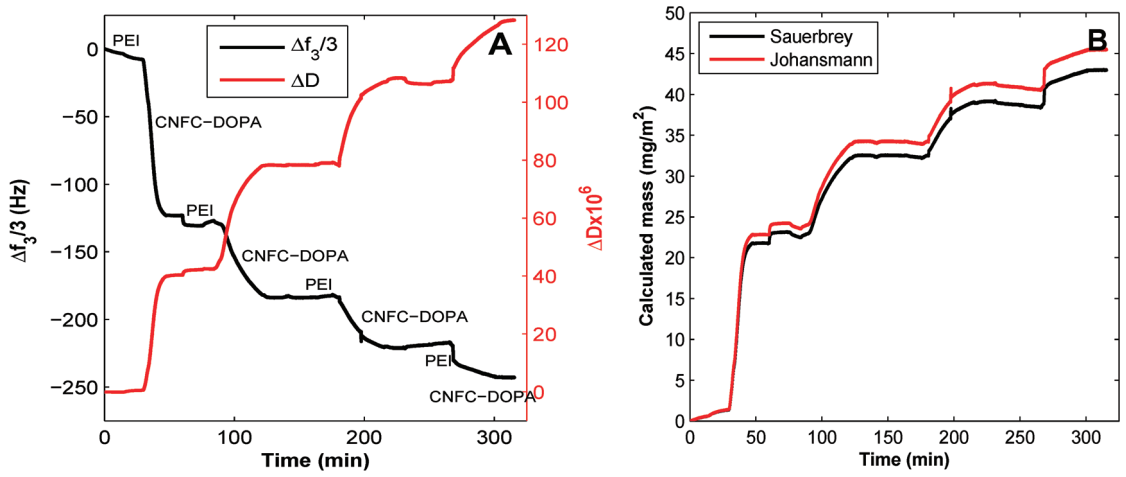

Figure 5. (a) Build-up of a (PEI/CNFC−DOPA)$_4$ multilayer film in the QCM-D. Left and right *y*-axes show the change in normalized frequency (considering the third overtone) and the change in energy dissipation, respectively. Each deposition step is indicated by the name of the added building block. (b) Total adsorbed mass of the (PEI/CNFC−DOPA)$_4$ multilayer film calculated using the Sauerbrey and Johannsmann models.

than that of unmodified CNFC. This can be attributed to the association of the nanofibrils. The association tendency of the CNFC−DOPA is also obvious when the autocorrelation curves for the modified and nonmodified nanofibril dispersions are compared, as in Figure 4a. The decay of the autocorrelation function is slower for the CNFC−DOPA particles, indicating that the modified fibrils diffuse more slowly than the nonmodified CNFC. The term association is used since there is no macroscopic phase separation of the CNFC−DOPA fibrils, which could be expected if there should be a complete aggregation of the fibrils. The fibrils are stable over time, and therefore the association is viewed as an association in a secondary minimum for the fibrils. Taking into account, as mentioned earlier, that the covalent conjugation is a site-specific modification, this aggregation tendency of CNFC−DOPA is probably due to a decrease in the number of free carboxyl groups in CNFC. However, since the measured ζ-potentials of pure CNFC and CNFC−DOPA were −50.7 and −36.7 mV, respectively, it is clear that not all the carboxylic groups were converted to their amide form and that some carboxyl groups were indeed left after the coupling reaction. This indicates that there should be a weak barrier against aggregation under salt-free conditions,[32] and it can therefore be suggested that the association found for the CNFC−DOPA is due to interactions between the fibrils caused by the DOPA functionality. The existence of free carboxyl groups is a prerequisite for the formation of LbL films of CNFC−DOPA and cationic polyelectrolytes. The association tendency of the CNFC−DOPA will influence the structure of multilayer films prepared using CNFC−DOPA, and it would be expected that PEI would be influenced by this coagulation behavior in liquid. This phenomenon is discussed in more detail later in the context of surface topography of the multilayer films.

LbLs of DOPA-Modified CNFC and PEI: Formation and Properties. One of the main ideas behind the present work was to form thin films of CNFC and both to strengthen these films internally *via* iron-ion-induced cross-linking and to increase their adhesion to different supports. It was therefore essential to establish whether an LbL structure could be formed with modified fibrils. As shown in Figure 5a, the consecutive deposition of CNFC−DOPA and PEI has been monitored using a quartz crystal microbalance with dissipation (QCM-D) technique[33] in which the change in oscillation frequency and energy dissipation are monitored *in situ* as a function of time. The total frequency decay for the (CNFC−DOPA/PEI)$_4$ (the subscript at the right of the parentheses denotes the number of deposition cycles) film was approximately the same as that of an LbL film prepared from the unmodified CNFC and PEI, as reported earlier.[9] However, the change in energy dissipation was roughly 3 times higher than that of (CNFC/PEI)$_4$, which can be attributed to the formation of more viscoelastic (soft) layers due to the relatively lower electrostatic interaction between CNFC−DOPA and PEI compared to that of pure CNFC−PEI multilayers. As shown in Figure 5b, the frequency change was transformed to the adsorbed mass using the Sauerbrey[33] and Johannsmann[34] models, and the total mass of the (PEI/CNFC−DOPA)$_4$ multilayer film was calculated as 43 and 46 mg m^{-2}. These results are in agreement with the previous findings of Karabulut *et al.*,[9] in which the adsorbed mass was found to be around 52 mg m^{-2} for the (PEI/CNFC)$_5$ film. It should be noted that the deposition of LbL building blocks is significantly dependent on the amount of charged groups, and it may not be possible to deposit the layers consecutively when the chemical grafting exceeds a certain level. In order to test this hypothesis, an experiment was performed in which the pure PEI was replaced with

its catechol-grafted version (PEI–CAT) prepared using 3,4-dihydroxycinnamic acid. It was found that there was only a very weak electrostatic interaction between CNFC–DOPA and PEI–CAT and that the layers formed were easily rinsed off with Milli-Q water. When the PEI–CAT was replaced with pure PEI, it was again possible to form a multilayer film by combining the pure PEI with CNFC–DOPA. (Further details are given in Figure S2.)

The swelling ability of the LbL films prepared from CNFC–DOPA and PEI was determined by recording the AFM images of $(CNFC–DOPA/PEI)_8$ film in air, Milli-Q water, and $FeCl_3$ solution (see Figure S3). The thickness of the $(CNFC–DOPA/PEI)_8$ film was measured as 130 nm when the sample was completely dry. The dry thickness measured by ellipsometry was consistent with that of monitored in AFM cross-section profiles. The thickness of a multilayer film prepared with CNFC–DOPA and PEI increased three times when the Milli-Q water was injected because of the penetration of the water molecules into the layers. Furthermore, the swelling of the LbL film increased even more when Milli-Q water was replaced with $FeCl_3$ solution, which reveals an additional swelling mechanism associated with Fe^{3+} ions. This phenomenon can be explained by the increase in the volume occupied by the DOPA molecules due to the formation of ionic coordination complexes and to a decreased interaction between the DOPA–NFC and the PEI when increasing the amount of multivalent ions within the LbL structure. The swelling of the films reached a plateau in 10–15 min after the injection of 1 mM $FeCl_3$ solution. In addition, the swelling of the $(CNFC–DOPA/PEI)_8$ film could be reversed by altering the liquid from the $FeCl_3$ solution to pure Milli-Q water, which shows that the ionic complex formation is reversible. All these observations concerning the ionic complex formation and its reversibility are in agreement with the findings of Zeng and Hwang *et al.*[26] in which the time- and Fe^{3+}-concentration-dependence of the bridging between DOPA-containing mfp-1 protein films have been discussed in terms of the reversibility of complex formation and adhesion. When a multilayer film containing CNFC–DOPA is compared with an mfp-1 protein film, however, the differences between a protein with 3D structure, which will be influenced substantially by salt addition, and cellulose fibrils and also the high DOPA content existing in the protein should be considered. A single layer of CNFC–DOPA film has been prepared by solvent-casting in 1 mM $FeCl_3$ solution in a polystyrene Petri dish to study the influence of water on the film integrity and wet adhesion. The dry CNFC–DOPA film adheres strongly to the Petri dish surface, while a dry film prepared using nonmodified fibrils could easily be peeled off. When 10 mL of pure water was poured into the Petri dishes, the CNFC–DOPA film kept its integrity and remained bonded to the Petri dish surface, whereas a pure CNFC film started to swell and float off in the water. It can therefore be concluded that the ionic complex formation between the DOPA and Fe^{3+} gives an additional wet stability to the films prepared using only modified nanofibrils containing no polyelectrolyte.

Surface Morphologies of the $(CNFC/PEI)_8$ and $(CNFC–DOPA/PEI)_8$ Multilayer Films. The surface morphologies of the LbL films of pure CNFC and CNFC–DOPA combined by PEI were assessed by tapping-mode AFM imaging. The random orientation of the nanofibrils was monitored for two types of multilayer films consisting of the same number of layer pairs. The average surface roughness expressed as rms roughness of the $(CNFC/PEI)_8$ film was 5 ± 0.5 nm, whereas that of the $(CNFC–DOPA/PEI)_8$ film was 8.5 ± 0.8 nm. As shown in Figure 6, the multilayer film prepared using grafted nanofibrils contains association structures leading to a slightly rougher film than that prepared with nonmodified cellulose nanofibrils, but large-scale flocs are definitely missing, supporting the fact that the DOPA modification leads to a weak association of the fibrils and not a large-scale aggregation. The increase in surface roughness can be attributed to the decrease of charged groups on the nanofibril surface, leading to a weak electrostatic repulsion and hence a nanofibrillar association on the silicon substrate. This behavior was more obvious in the case of the multilayer films prepared using PEI–CAT and CNFC–DOPA, in which the electrostatic interaction was very weak, and the LbL film buildup was therefore not possible due to the desorption of weakly attached layers. The final morphology of such a film is rather disordered, island-like structures remaining after the rinsing steps, but still single fibrils can be identified on the surfaces, showing that there is not a large-scale aggregation due to the DOPA modification. All these observations show that the degree of chemical functionalization of the nanofibrils has a significant effect on both the colloidal stability of the CNFC–DOPA and its adsorption properties.

Wet Adhesion Measurements of the $(PEI/CNFC)_8$ and $(PEI/CNFC–DOPA)_8$ Films. The influence of metal–DOPA complex formation on the wet adhesion of the modified CNFC to inorganic substances was studied with the aid of colloidal probe AFM measurements.[35,36] In this investigation, a bare silica particle was brought close to the $(PEI/CNFC–DOPA)_8$ and $(PEI/CNFC)_8$ films in Milli-Q water and 1 mM NaCl and 1 mM $FeCl_3$ solutions. Figure 7 shows typical force–distance curves between the silica particle and the $(PEI/CNFC–DOPA)_8$ film in these different solutions. The adhesive forces between the silica particle and $(PEI/CNFC–DOPA)_8$ film were similar and relatively low in NaCl solution and Milli-Q water (F_{ad}/R -3.8 ± 2.0 and -4.8 ± 0.67 mN m^{-1} for 1 mM NaCl solution and Milli-Q water, respectively). When $FeCl_3$ solution was introduced, adhesion increased approximately three times (F_{ad}/R -9.97 ± 0.49 mN m^{-1})

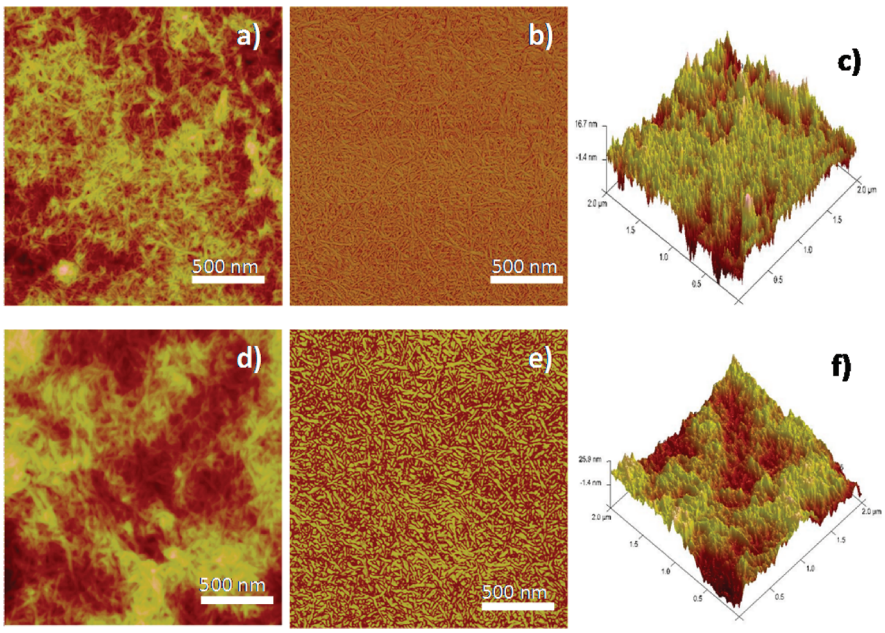

Figure 6. AFM tapping-mode (a) height, (b) phase, and (c) 3D images of $(PEI/CNFC)_8$ film. (d, e, and f) Height, phase, and 3D images of the $(PEI/CNFC-DOPA)_8$ film. The scanned area was 2 × 2 μm for all the images, and the *z* range is 25 nm.

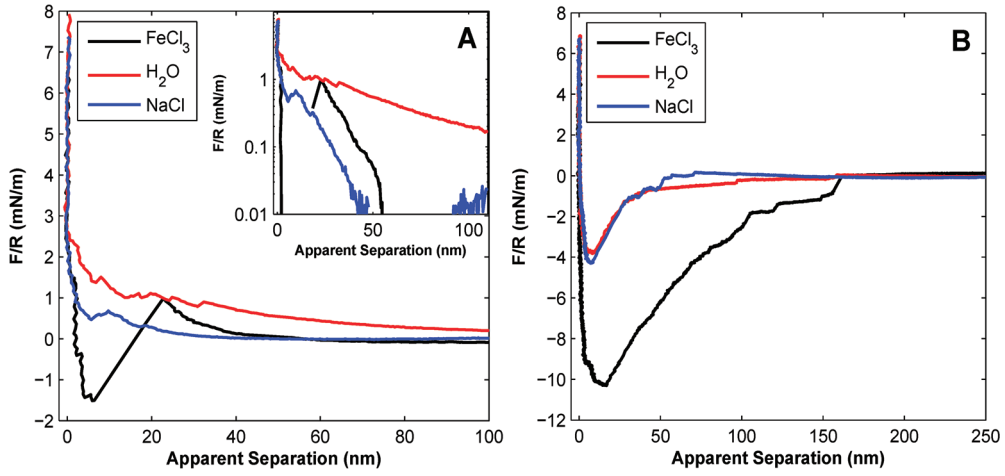

Figure 7. Normalized force curves recorded between the $(PEI/CNFC-DOPA)_8$ film and silica particles upon (a) approach and (b) withdrawal in Milli-Q water, 1 mM NaCl solution, and 1 mM $FeCl_3$ solution.

measured 10 min after the injection of the $FeCl_3$ solution. This increase in adhesion indicates that Fe^{3+} ions contribute to the wet adhesion by forming DOPA–metal complexes. Despite the fact that the surfaces are not symmetric in our experiments and that the possibility of conformational changes is much higher for mfp-1 protein, these results are in agreement with the previous findings of Zeng *et al.* in which the adhesion forces between mfp-1 protein-coated surfaces were found to be between −8 and −20 mN m^{-1} depending on the contact time.[26] It can also be seen that the separation between the silica probe and the $(PEI/CNFC-DOPA)_8$ film occurred in multiple steps in the presence of Fe^{3+} ions, and the adhesion distance was approximately 5 times greater than in NaCl solution and water. To test if the Fe^{3+} ions could improve the adhesion of the DOPA-modified CNFC, further adhesion measurements were performed at the same Fe^{3+} concentration with a reference LbL film, $(PEI/CNFC)_8$, prepared using nongrafted fibrils, as shown in Figure 8. These results show no significant wet adhesion between the silica colloidal probe and the $(PEI/CNFC)_8$ films in the presence of water and Fe^{3+} ions. A weaker electrostatic repulsion was observed in $FeCl_3$ compared to the $(PEI/CNFC)_8$ film, which can be attributed to the effect of increased ionic strength, providing a screening against the charges of the approaching surfaces. Interestingly there is a jump into contact for the $(PEI/CNFC-DOPA)_8$ film in the presence of the Fe^{3+} from a separation of approximately 20 nm, which is attributed to a bridging force due to the formation of the DOPA–metal complex.

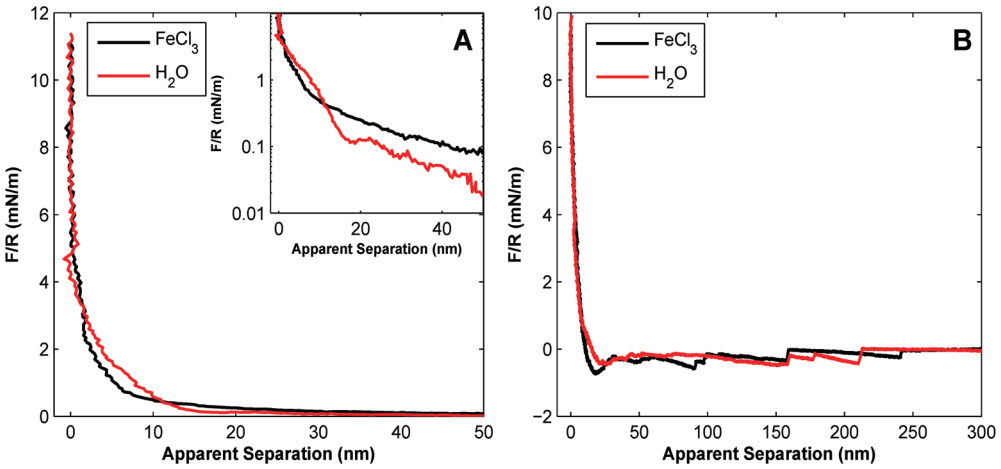

Figure 8. Normalized force curves recorded between the $(PEI/CNFC)_8$ film and silica particles upon (a) approach and (b) withdrawal in Milli-Q water and 1 mM $FeCl_3$ solution.

CONCLUSIONS

A new generation of wood-fiber-based cellulose nanofibrils was prepared by grafting 3,4-dihydroxyphenylalanine to the nanofibrils using standard carbodiimide chemistry. Although this grafting technique has been used in biological applications, especially in peptide and protein sciences, it is the first time to our knowledge that a low-cost raw material obtained from wood has been chemically modified with an organic molecule bearing a functionality in order to prepare adhesive surface coatings on hydrophobic substances. Robust, adhesive, and wet-stable multilayer films of CNFC–DOPA and PEI were formed, and the LbL film properties were evaluated in terms of their structure and adhesion characteristics. Since the DOPA grafting leads to a reduction in the amount of carboxyl groups on the fibrils, the modification leads to a slight loss in colloidal stability of the fibrils when the degree of substitution of DOPA is increased. Nevertheless, the charge of the CNFC–DOPA used was high enough to allow for a steady buildup of LbL films of CNFC–DOPA and PEI. The LbL films prepared in this way showed a significant wet adhesion to a silica probe in AFM force measurements in the presence of Fe^{3+} ions, indicating that DOPA–metal ion complex formation stimulates the adhesion between the DOPA-containing LbL films and inorganic surfaces. The DOPA-modified CNFC films prepared by solvent casting formed very stable and adhesive thin coatings on polystyrene surfaces when they were cross-linked with Fe^{3+} ions. The CNFC–DOPA coatings did not peel off and deform when they were dipped into water, whereas films of pure CNFCs exhibited a weak dry and wet stability on a polystyrene substrate. In this respect, our biomimetic approach with a renewable raw material offers a promising way of preparing adhesive coatings on a large variety of surfaces. The preparation of adhesive nanocoatings using not only DOPA but also other functional macromolecules bearing primary amines could open up new possibilities, combined with a relatively low-cost and "green" raw material such as CNFC.

EXPERIMENTAL SECTION

Instrumentation. A Perkin-Elmer Spectrum 2000 FTIR spectrometer with ATR accessory and a Shimadzu UV-2550 spectrophotometer were used to characterize the covalent conjugate formation of CNFC and DOPA. The consecutive deposition of PEI and CNFC–DOPA on SiO_2 surfaces was monitored with QCM-D (Q-Sense AB, Västra Frölunda, Sweden) by a method similar to that used in earlier measurements.[9]

The average size and ζ-potential of the modified nanofibrils were measured using a dynamic light scattering equipment (Nano ZS-ZEN3600, Malvern Instruments Ltd., Worcestershire, UK).[32] The surface morphology and roughness of the multilayer films were studied with tapping-mode AFM (Picoforce SPM, Veeco, Santa Barbara, CA, USA). All measurements were made with a maximum scan rate of 1 Hz using 512 samples per line. Standard noncontact silicon cantilevers (RTESP, Veeco, Santa Barbara, CA, USA) with spring constants of 40 N m^{-1} were used. The scanned surface area was 2×2 μm^2 for each sample.

The wet adhesion measurements have been made using the AFM colloidal probe technique[35,36] in which a Nanoscope IIIa Picoforce system (Veeco Instrument Ltd., Santa Barbara, CA, USA) was used in the contact mode by ramping the probe up and down relative to the sample surface. A borosilicate particle (Duke Scientific Corp., Palo Alto, CA, USA) with a diameter of 10 ± 1 μm was glued to a NCS12 tipless silica cantilever (MikroMasch, San Jose, CA, USA) with a typical length of 250 μm, a width of 35 μm, and a typical spring constant of 0.8 N m^{-1} selected according to the manufacturer's recommendation.[37] The spring constants of the cantilevers were determined in air using the calibration software AFM TuneIT v2.5 (ForceIT, Sweden) based on hydrodynamic damping.[38,39]

Chemicals and Materials. A carboxymethylated NFC dispersion was prepared by Innventia AB, Stockholm, Sweden, according to a procedure described by Wågberg *et al.*[5] In brief, a dispersion of never-dried cellulose fibers obtained from a commercial softwood sulfite dissolving pulp (Domsjö Fabriker AB, Domsjö, Sweden) was dispersed in deionized water at 10 000 revolutions

in an ordinary laboratory slusher. The fibers were then treated with 2 wt % of monochloroacetic acid in 2-propanol. Following the carboxymethylation step, the fibers were filtered, washed with water/acetic acid/water, and impregnated with $NaHCO_3$ solution (4 wt %) in order to convert the carboxyl groups into their sodium form. The fibers were carefully washed with deionized water to remove excess salt after this treatment. The fibers were then homogenized using a high-pressure fluidizer (Microfluidizer M-110EH, Microfluidics Corp.). The nanofibril dispersions obtained from the homogenization were dispersed by ultrasonication prior to use. In order to remove the fibril aggregates and contaminants from the sonication probe, the dispersion was centrifuged at 10 000 rpm, and only the supernatant was used in the experiments. Dopamine hydrochloride, *N*-(3-dimethylaminopropyl)-*N*′-ethylcarbodiimide hydrochloride, *N*-hydroxysuccinimide (98%), and iron(III) chloride were purchased from Sigma-Aldrich. PEI, with the commercial name LupasolP (50% aqueous solution, M_w = 750 000 g mol^{-1} according to the supplier), was kindly supplied by BASF, Ludwigshafen, Germany, and dialyzed for four days against Milli-Q water prior to use. Silicon wafers (MEMC Electronic Materials, Inc., Novara, Italy) were cut into small pieces (2 × 6 cm^2) and precleaned by dipping into piranha solution (3:1 mixture (v/v) of H_2O_2 and concentrated H_2SO_4) for 30 min followed by extensive rinsing with ethanol (95%) and Milli-Q water. The clean wafers were then dried under a nitrogen flow. Silicon wafers were placed in the plasma cleaner for 2 min at medium power (10 W) followed by immersion in 0.1 M NaOH. In the QCM-D experiments, AT-cut quartz crystal sensors (Q-Sense AB, Västra Frölunda, Sweden) with a 50 nm thick SiO_2 layer (QSX 303) were used, and the crystals were cleaned with an ethanol/Milli-Q water mixture followed by 2 min of UV plasma treatment at medium power.

Preparation of DOPA-Grafted Cellulose Nanofibrils. A 100 mL amount of 1.4 g L^{-1} NFC dispersion was mixed with 100 mL of PBS buffer, and the pH of the mixture was adjusted to pH = 5 by adding 0.1 M HCl. To this mixture, 0.06 mmol of DOPA, 0.1 mmol of *N*-(3-dimethylaminopropyl)-*N*′-ethylcarbodiimide hydrochloride, and 0.1 mmol of *N*-hydroxysuccinimide were added, and the pH was maintained at pH = 5 while the mixture was stirred vigorously for 6 h. The mixture was dialyzed for 24 h in PBS buffer and then for five days in Milli-Q water. After dialysis, a small amount of the DOPA-grafted nanofibril dispersion was freeze-dried overnight for the FTIR analysis. The UV−vis spectrum of a diluted dispersion of CNFC−DOPA conjugate was recorded in Milli-Q water over a wavelength range of 200−400 nm.

Consecutive Deposition of CNFC−DOPA and PEI on a Solid Surface. An automatic dipping robot equipped with a nitrogen drying unit (StratoSequence VI, nanoStrata Inc., Tallahassee, FL, USA) was used to prepare the multilayer films of CNFC−DOPA and PEI. CNFC−DOPA and PEI were adsorbed by alternately dipping the silicon substrate (2 × 6 cm^2) into the PEI solution and the CNFC−DOPA dispersion followed by rinsing with Milli-Q water for 3 min and drying with nitrogen gas for 30 s after the final rinsing step of each layer. The concentration of the CNFC−DOPA dispersion and PEI solution was 1 g L^{-1}, and 50 mM NaCl was added to the PEI solution. The pH of the PEI solution was adjusted to pH = 8 with 1 N HCl, while that of the CNFC dispersion was kept constant at pH = 7. The Milli-Q water used for rinsing the substrates was replaced with fresh water after three deposition cycles in order to prevent any unevenly distributed complex formation.

Conflict of Interest: The authors declare no competing financial interest.

Acknowledgment. This work was financially supported by the European Commission (EU Seventh Framework Programme) under Contract No. 214660, SustainComp Project. The Wallenberg Wood Science Centre (WWSC) is also acknowledged for financing L.W.

Supporting Information Available: A document containing the following information: digital photographs of the self-supporting CNFC film and the coating of CNFC−DOPA on a polystyrene surface; change in oscillation frequency and energy dissipation for the CNFC−DOPA and PEI−CAT multilayer film; AFM thickness profiles of the $(PEI/CNFC-DOPA)_8$ film in water and NaCl and $FeCl_3$ solutions; chemical structures of 3,4-Ddihydroxycinnamic acid (CAT) and PEI−CAT conjugate; coupling mechanism of CNFC and DOPA *via* carbodiimide chemistry; normalized force curves recorded between $(PEI/CNFC)_{7.5}$ film and silica particles; UV−vis spectra of the CNFC−DOPA conjugates prepared by adding different amounts of DOPA to the reaction mixture; QCM-D adsorption curves of the $(PEI/CNFC-DOPA)_4$ film at pH = 3.5. This material is available free of charge via the Internet at http://pubs.acs.org.

REFERENCES AND NOTES

1. Meyers, M. A.; Chen, P. Y.; Lin, A. Y. M.; Seki, Y. Biological Materials: Structure and Mechanical Properties. *Prog. Mater Sci.* **2008**, *53*, 1–206.
2. Eichhorn, S. J. Cellulose Nanowhiskers: Promising Materials for Advanced Applications. *Soft Matter* **2010**, *7*, 303–315.
3. Klemm, D.; Kramer, F.; Moritz, S.; Lindström, T.; Ankerfors, M.; Gray, D.; Dorris, A. Nanocelluloses: A New Family of Nature-Based Materials. *Angew. Chem., Int. Ed.* **2011**, *50*, 5438–5466.
4. Pääkkö, M.; Ankerfors, M.; Kosonen, H.; Nykanen, A.; Ahola, S.; Österberg, M.; Ruokolainen, J.; Laine, J.; Larsson, P. T.; Ikkala, O.; *et al.* Enzymatic Hydrolysis Combined with Mechanical Shearing and High-Pressure Homogenization for Nanoscale Cellulose Fibrils and Strong Gels. *Biomacromolecules* **2007**, *8*, 1934–1941.
5. Wågberg, L.; Decher, G.; Norgren, M.; Lindström, T.; Ankerfors, M.; Axnäs, K. The Build-up of Polyelectrolyte Multilayers of Microfibrillated Cellulose and Cationic Polyelectrolytes. *Langmuir* **2008**, *24*, 784–795.
6. Henriksson, M.; Berglund, L. A.; Isaksson, P.; Lindström, T.; Nishino, T. Cellulose Nanopaper Structures of High Toughness. *Biomacromolecules* **2008**, *9*, 1579–1585.
7. Ishii, D.; Saito, T.; Isogai, A. Viscoelastic Evaluation of Average Length of Cellulose Nanofibers Prepared by Tempo-Mediated Oxidation. *Biomacromolecules* **2011**, *12*, 548–550.
8. Cranston, E. D.; Gray, D. G. Model Cellulose I Surfaces: A Review. In *Model Cellulosic Surfaces*; Roman, M., Ed.; American Chemical Society: Washington, DC, 2009; Vol. 1019, pp 75−93.
9. Karabulut, E.; Wågberg, L. Design and Characterization of Cellulose Nanofibril-Based Freestanding Films Prepared by Layer-by-Layer Deposition Technique. *Soft Matter* **2011**, *7*, 3467–3474.
10. Sehaqui, H.; Liu, A.; Zhou, Q.; Berglund, L. A. Fast Preparation Procedure for Large, Flat Cellulose and Cellulose/Inorganic Nanopaper Structures. *Biomacromolecules* **2010**, *11*, 2195–2198.
11. Sehaqui, H.; Salajkova, M.; Zhou, Q.; Berglund, L. A. Mechanical Performance Tailoring of Tough Ultra-High Porosity Foams Prepared from Cellulose I Nanofiber Suspensions. *Soft Matter* **2010**, *6*, 1824–1832.
12. Aulin, C.; Netrval, J.; Wågberg, L.; Lindström, T. Aerogels from Nanofibrillated Cellulose with Tunable Oleophobicity. *Soft Matter* **2010**, *6*, 3298–3305.
13. Korhonen, J. T.; Kettunen, M.; Ras, R. H. A.; Ikkala, O. Hydrophobic Nanocellulose Aerogels as Floating, Sustainable, Reusable, and Recyclable Oil Absorbents. *ACS Appl. Mater. Interfaces* **2011**, *3*, 1813–1816.
14. Liu, A.; Walther, A.; Ikkala, O.; Belova, L.; Berglund, L. A. Clay Nanopaper with Tough Cellulose Nanofiber Matrix for Fire Retardancy and Gas Barrier Functions. *Biomacromolecules* **2011**, *12*, 633–641.
15. Laaksonen, P.; Walther, A.; Malho, J.-M.; Kainlauri, M.; Ikkala, O.; Linder, M. B. Genetic Engineering of Biomimetic Nanocomposites: Diblock Proteins, Graphene, and Nanofibrillated Cellulose. *Angew. Chem., Int. Ed.* **2011**, *50*, 8688–8691.
16. Waite, J. H.; Tanzer, M. L. Polyphenolic Substance of Mytilus-Edulis - Novel Adhesive Containing L-Dopa and Hydroxyproline. *Science* **1981**, *212*, 1038–1040.

17. Burzio, L. A.; Waite, J. H. Cross-Linking in Adhesive Quinoproteins: Studies with Model Decapeptides. *Biochemistry* **2000**, *39*, 11147–11153.
18. Carrington, E.; Gosline, J. M. Mechanical Design of Mussel Byssus: Load Cycle and Strain Rate Dependence. *Am. Malacol. Bull.* **2004**, *18*, 135–142.
19. Harrington, M. J.; Waite, J. H. Ph-Dependent Locking of Giant Mesogens in Fibers Drawn from Mussel Byssal Collagens. *Biomacromolecules* **2008**, *9*, 1480–1486.
20. Waite, J. H.; Qin, X. X. Polyphosphoprotein from the Adhesive Pads of Mytilus Edulis. *Biochemistry* **2001**, *40*, 2887–2893.
21. Ochs, C. J.; Hong, T.; Such, G. K.; Cui, J.; Postma, A.; Caruso, F. Dopamine-Mediated Continuous Assembly of Biodegradable Capsules. *Chem. Mater.* **2011**, *23*, 3141–3143.
22. Sever, M. J.; Weisser, J. T.; Monahan, J.; Srinivasan, S.; Wilker, J. J. Metal-Mediated Cross-Linking in the Generation of a Marine-Mussel Adhesive. *Angew. Chem., Int. Ed.* **2004**, *43*, 448–450.
23. Holten-Andersen, N.; Fantner, G. E.; Hohlbauch, S.; Waite, J. H.; Zok, F. W. Protective Coatings on Extensible Biofibres. *Nat. Mater.* **2007**, *6*, 669–672.
24. Holten-Andersen, N.; Mates, T. E.; Toprak, M. S.; Stucky, G. D.; Zok, F. W.; Waite, J. H. Metals and the Integrity of a Biological Coating: The Cuticle of Mussel Byssus. *Langmuir* **2009**, *25*, 3323–3326.
25. Harrington, M. J.; Masic, A.; Holten-Andersen, N.; Waite, J. H.; Fratzl, P. Iron-Clad Fibers: A Metal-Based Biological Strategy for Hard Flexible Coatings. *Science* **2010**, *328*, 216–220.
26. Zeng, H.; Hwang, D. S.; Israelachvili, J. N.; Waite, J. H. Strong Reversible Fe^{3+}-Mediated Bridging between Dopa-Containing Protein Films in Water. *Proc. Natl. Acad. Sci. U. S. A.* **2010**, *107*, 12850–12853.
27. Lee, H.; Lee, Y.; Statz, A. R.; Rho, J.; Park, T. G.; Messersmith, P. B. Substrate-Independent Layer-by-Layer Assembly by Using Mussel-Adhesive-Inspired Polymers. *Adv. Mater.* **2008**, *20*, 1619–1623.
28. Nakajima, N.; Ikada, Y. Mechanism of Amide Formation by Carbodiimide for Bioconjugation in Aqueous-Media. *Bioconjugate Chem.* **1995**, *6*, 123–130.
29. Staros, J. V.; Wright, R. W.; Swingle, D. M. Enhancement by N-Hydroxysulfosuccinimide of Water-Soluble Carbodiimide-Mediated Coupling Reactions. *Anal. Biochem.* **1986**, *156*, 220–222.
30. Barreto, W. J.; Ponzoni, S.; Sassi, P. A Raman and UV-Vis Study of Catecholamines Oxidized with Mn^{3+}. *Spectrochim. Acta A* **1999**, *55*, 65–72.
31. Vikkula, A.; Valkama, J.; Vuorinen, T. Formation of Aromatic and Other Unsaturated End Groups in Carboxymethyl Cellulose during Hot Alkaline Treatment. *Cellulose* **2006**, *13*, 593–600.
32. Fall, B. A.; Lindström, B. S.; Sundman, O.; Ödberg, L.; Wågberg, L. Colloidal Stability of Aqueous Nanofibrillated Cellulose Dispersions. *Langmuir* **2011**, *27*, 11332–11338.
33. Sauerbrey, G. Z. Verwendung Von Schwingquarzen Zur Wägung Dünner Schichten Und Zur Mikrowägung. *Z. Phys.* **1959**, *155*, 206–222.
34. Johannsmann, D.; Embs, F.; Willson, C. G.; Wegner, G.; Knoll, W. Viscoelastic Properties of Thin-Films Probed with a Quartz Crystal Resonator. *Makromol. Chem-M. Symp.* **1991**, *46*, 247–251.
35. Ducker, W. A.; Senden, T. J.; Pashley, R. M. Direct Measurement of Colloidal Forces Using an Atomic Force Microscope. *Nature* **1991**, *353*, 239–241.
36. Ducker, W. A.; Senden, T. J.; Pashley, R. M. Measurement of Forces in Liquids Using a Force Microscope. *Langmuir* **1992**, *8*, 1831–1836.
37. Thormann, E.; Pettersson, T.; Claesson, P. M. How to Measure Forces with Atomic Force Microscopy without Significant Influence from Nonlinear Optical Lever Sensitivity. *Rev. Sci. Instrum.* **2009**, *80*, 093701.
38. Pettersson, T.; Nordgren, N.; Rutland, M. W. Comparison of Different Methods to Calibrate Torsional Spring Constant and Photodetector for Atomic Force Microscopy Friction Measurements in Air and Liquid. *Rev. Sci. Instrum.* **2007**, *78*, 093702.
39. Sader, J. E.; Chon, J. W. M.; Mulvaney, P. Calibration of Rectangular Atomic Force Microscope Cantilevers. *Rev. Sci. Instrum.* **1999**, *70*, 3967–3969.